

## Geometry matters: inverse cytotoxic relationship for *cis/trans*-Ru(II) polypyridyl complexes from *cis/trans*-[PtCl<sub>2</sub>(NH<sub>3</sub>)<sub>2</sub>]

Erin Wachter,<sup>a,†</sup> Ana Zamora,<sup>b,†</sup> David K. Heidary,<sup>a</sup> José Ruiz<sup>b</sup> and Edith C. Glazer<sup>a,\*</sup>

<sup>a</sup>Department of Chemistry, University of Kentucky, Lexington, KY 40506, United States

<sup>b</sup>Departamento de Química Inorganica and Regional Campus of International Excellence "Campus Mare Nostrum", Universidad de Murcia, and Institute for Bio-Health Research of Murcia (IMIB-Arrixaca), E-30071 Murcia, Spain

<sup>†</sup>Authors contributed equally to this work.

### Supporting Information

1. Instrumentation
2. Materials
3. Synthesis
4. Thermal Exchange Kinetics
5. DNA Gel Electrophoresis
6. Cell Cytotoxicity
7. Cellular Uptake
8. Additional Figures and Tables

**Table S1.** Conditions for thermal exchange kinetics.

**Figure S1.** Thermal exchange of **1a** followed by UV/Vis absorption spectroscopy in different aqueous solutions.

**Figure S2.** Thermal exchange of **1b** followed by UV/Vis absorption spectroscopy in different aqueous solutions.

**Figure S3.** Thermal exchange of **2a** followed by UV/Vis absorption spectroscopy in different aqueous solutions.

**Figure S4.** Thermal exchange of **2b** followed by UV/Vis absorption spectroscopy in different aqueous solutions.

**Table S2.** Half-lives of thermal exchange for **1a**.

**Table S3.**  $\Delta_{\text{abs}}$  of thermal exchange for **1b**.

**Table S4.**  $\Delta_{\text{abs}}$  of thermal exchange for **2a**.

**Table S5.**  $\Delta_{\text{abs}}$  of thermal exchange for **2b**.

**Figure S5.** Cellular accumulation and % uptake of **1a** and **2a** in HL-60 cells

**Figure S6.** ESI-MS for the thermal reaction of **1a** with imidazole.

**Figure S7.** ESI-MS for the thermal reaction of **2a** with imidazole.

**Figure S8.** HPLC analysis for the thermal reaction of **1a** and **2a** with imidazole.

**Figure S9.** <sup>1</sup>H-NMR in CD<sub>3</sub>CN for **1b**.

**Figure S10.** <sup>13</sup>C-NMR in CD<sub>3</sub>CN for **1b**.

**Figure S11.** HPLC purity and UV/Vis for **1b**.

**Figure S12.** <sup>1</sup>H-NMR in CD<sub>3</sub>CN for **2b**.

**Figure S13.** <sup>13</sup>C-NMR in CD<sub>3</sub>CN for **2b**.

**Figure S14.** HPLC purity and UV/Vis for **2b**.

9. References

## 1. Instrumentation:

A Varian Mercury spectrometer was used to obtain  $^1\text{H}$  NMR spectra (400 MHz) and  $^{13}\text{C}$  NMR spectra (100 MHz).  $^1\text{H}$  NMR chemical shifts are reported relative to the solvent peak ( $\text{CD}_3\text{CN} - \delta$  1.94 or  $\text{CDCl}_3 - \delta$  7.24). The  $^{13}\text{C}$  chemical shifts are referenced to  $\text{CD}_3\text{CN}$  at 1.39. Electrospray ionization (ESI) mass spectra were obtained using a Varian 1200L mass spectrometer at the University of Kentucky Environmental Research Training Laboratory (ERTL). Absorption spectra for the extinction coefficient determination were obtained on a Cary 60 UV/Vis spectrophotometer. Compound purity was determined with an Agilent 1100 Series HPLC using a previously reported method.<sup>1</sup> Full spectrum absorbance readings to determine the thermal exchange were completed using a BMG Labtech FLUOstar Omega microplate reader. Agarose gels were digitally imaged using a BioRad ChemiDoc System. Cell viability was measured using a SpectraFluor Plus Plate Reader (Tecan) equipped with a 485/590 filter. Uptake experiments were performed using a Varian 880Z graphite furnace atomic absorption spectrometer with Zeeman background correction, a palladium matrix modifier and detection using a 349.9 nm lamp. Flow cytometry experiments were run on a Becton-Dickinson LSRII Flow Cytometer and analyzed using FlowJo.

## 2. Materials:

Chemicals used for synthesis were purchased from VWR or Fisher Scientific and used without further purification. *cis*- $\text{Ru}(\text{bpy})_2\text{Cl}_2$  (**1a**) was purchased from Strem chemicals, dissolved in DMSO, and stored at  $-20^\circ\text{C}$ . Cisplatin and transplatin were used as control compounds for biological studies. Care was taken to keep the compounds in the dark for both synthesis and biological characterization. Media used for cytotoxicity studies were purchased from Invitrogen. Cancer cell lines were obtained from ATCC.

## 3. Synthesis:

***cis*-[Ru(bpy)(py)<sub>2</sub>](PF<sub>6</sub>)<sub>2</sub> (**1b**):** To a suspension of  $\text{Ru}(\text{bpy})_2\text{Cl}_2 \cdot 2\text{H}_2\text{O}$  (106 mg, 0.204 mmol) in  $\text{EtOH}:\text{H}_2\text{O}$  (1:1) an excess of pyridine (375  $\mu\text{L}$ , 4.60 mmol) was added under  $\text{N}_2$ . The resulting mixture was refluxed at  $90^\circ\text{C}$  for 6 hrs. After cooling the red solution to  $22^\circ\text{C}$ , 1–2 mL of a saturated aqueous  $\text{KPF}_6$  solution was added to produce a red precipitate that was then extracted into  $\text{CH}_2\text{Cl}_2$  (3 x 40 mL). The organic phase was further purified by flash chromatography ( $\text{SiO}_2$  eluting at 89:11:0.7 acetonitrile/water/saturated  $\text{KNO}_3$ ). The solvent was removed under vacuum, and the complex was converted to  $\text{PF}_6^-$  salt. The product was obtained in 70% yield (132 mg) as a red solid.  $^1\text{H}$  NMR ( $\text{CD}_3\text{CN}$ , 400 MHz):  $\delta$  = 8.92 (d,  $J$  = 5.6 Hz, 2H), 8.36 (d,  $J$  = 7.9 Hz, 2H), 8.30–8.26 (m, 6H), 8.13 (td,  $J$  = 7.9, 1.4 Hz, 2H), 7.94–7.89 (m = 4H), 7.85 (tt,  $J$  = 7.7, 1.5 Hz, 2H), 7.77 (ddd,  $J$  = 7.6, 5.7, 1.4 Hz, 2H), 7.36 (ddd,  $J$  = 7.4, 5.9, 1.3 Hz, 2H), 7.31–7.28 (m, 4H);  $^{13}\text{C}$  NMR ( $\text{CD}_3\text{CN}$ , 100 MHz): 158.65, 158.60, 154.62, 153.74, 153.40, 139.10, 138.96, 138.65, 128.95, 128.64, 127.19, 125.03, 124.75; Purity by HPLC: 99.9 % by area; UV/Vis in  $\text{CH}_3\text{CN}$ ,  $\lambda_{\text{max}}$  ( $\epsilon \text{ M}^{-1} \text{ cm}^{-1}$ ) = 240 (34000), 290 (56400), 335 nm (15800), 450 (1000); ESI MS calcd for  $\text{C}_{30}\text{H}_{26}\text{N}_6\text{Ru}$ :  $[\text{M}^{2+} \cdot \text{PF}_6^-]^+$  717.1,  $[\text{M-py}]^{2+}$  246.6,  $[\text{M-2 py}]^{2+}$  207.1, found 717.2  $[\text{M}^{2+} \cdot \text{PF}_6^-]^+$ , 246.3  $[\text{M-py}]^{2+}$ , 206.9  $[\text{M-2 py}]^{2+}$ .

**2,2':6',2'':6'',2'''-quaterpyridine (qpy):** A mixture of  $\text{K}_2\text{CO}_3$  (176 mg, 1.28 mmol),  $\text{Pd}(\text{OAc})_2$  (43 mg, 0.64 mmol),  $\text{NBu}_4\text{Br}$  (206.3 mg, 0.64 mmol) and 6-bromobipyridine

(300 mg, 1.28 mmol) in DMF (2 mL) was stirred under N<sub>2</sub> atmosphere for a few minutes at 115 °C. Then, isopropanol (8 mL) was added to the orange solution and the final mixture was stirred at 115 °C for 3h. After cooling to 22 °C, water and ether were added and the organic phase was extracted and dried over MgSO<sub>4</sub>. The solvent was removed under vacuum to obtain a pale yellow solid. Yield: 242 mg (61%). <sup>1</sup>H NMR (CDCl<sub>3</sub>, 400 MHz): δ = 8.75–8.72 (m, 2H), 8.70–8.66 (m, 4H), 8.51 (dd, *J* = 8.0, 1.2 Hz, 2H), 8.01 (t, *J* = 8.0 Hz, 2H), 7.91 (td, *J* = 8.0, 1.6 Hz, 2H), 7.39–7.35 (m, 2H). ESI MS calcd for C<sub>20</sub>H<sub>14</sub>N<sub>4</sub>: [L•H]<sup>+</sup> 310.12, found 311.1 [L•H]<sup>+</sup>.

*trans*-Ru(qpy)Cl<sub>2</sub>•3.5 H<sub>2</sub>O (**2a**) was prepared by literature method.<sup>2</sup>

The following complex was synthesized in order to confirm **2a** was mononuclear:

*trans*-[Ru(qpy)(py)<sub>2</sub>](PF<sub>6</sub>)<sub>2</sub> (**2b**): To a suspension of Ru(qpy)Cl<sub>2</sub>•3.5 H<sub>2</sub>O (50 mg, 0.092 mmol) in EtOH:H<sub>2</sub>O (4:1) an excess of pyridine (741 μL, 9.20 mmol) was added under N<sub>2</sub>. The resulting mixture was refluxed at 85 °C overnight. After cooling the red solution to 22 °C, 1–2 mL of a saturated aqueous KPF<sub>6</sub> solution was added to obtain a red precipitate that was extracted with CH<sub>2</sub>Cl<sub>2</sub>/CH<sub>3</sub>CN (3 x 10 mL). The organic phase was further purified by flash chromatography (SiO<sub>2</sub> eluting at 80:20:0.1 acetonitrile/water/saturated KNO<sub>3</sub>). The solvent was removed under vacuum, and the complex was converted to PF<sub>6</sub><sup>-</sup> salt. The product was obtained in 92% yield (74 mg) as a red solid. <sup>1</sup>H NMR (CD<sub>3</sub>CN, 400 MHz): δ = 9.70 (dd, *J* = 6.4, 0.8 Hz, 2H), 8.57 (d, *J* = 8.4 Hz, 2H), 8.29 (d, *J* = 7.6 Hz, 2H), 8.20 (d, *J* = 8.0 Hz, 2H), 8.16–8.08 (m, 4H), 7.95–7.91 (m, 6H), 7.58–7.54 (m, 2H), 7.03 (t, *J* = 7.2 Hz, 2H); <sup>13</sup>C NMR (CD<sub>3</sub>CN, 100 MHz): 160.49, 160.41, 159.22, 155.34, 152.16, 141.13, 138.94, 136.92, 130.52, 126.69, 126.28, 125.13, 125.07; Purity by HPLC: 99.9 % by area; UV/Vis in CH<sub>3</sub>CN, λ<sub>max</sub> (ε M<sup>-1</sup> cm<sup>-1</sup>) = 290 (61100), 330 (32800), 350 nm (35800), 460 (5900), 530 (7000); ESI MS calcd for C<sub>30</sub>H<sub>24</sub>N<sub>6</sub>Ru: [M<sup>2+</sup>•PF<sub>6</sub><sup>-</sup>]<sup>+</sup> 715.07, [M]<sup>2+</sup> 285.05, [M-py]<sup>2+</sup> 245.54, [M-2py]<sup>2+</sup> 206.02, found 715.2 [M<sup>2+</sup>•PF<sub>6</sub><sup>-</sup>]<sup>+</sup>, 284.9 [M]<sup>2+</sup>, 245.4 [M-py]<sup>2+</sup>, 205.8 [M-2py]<sup>2+</sup>.

**Note:** Ru(II) complexes with chloride ligands were prepared as stock solutions in DMSO immediately prior to testing. These complexes can exchange ligands over time.

#### 4. Thermal Exchange Kinetics

The thermal exchange kinetics of 40 μM **1a**, **1b**, **2a**, and **2b** were measured in 96-well plate for 15 hours at 37 °C. Each condition was run in triplicate and the data was fit to either a one phase or two phase decay equation using Prism software. Table S1 gives the experimental conditions used in all studies.

To determine how many Cl<sup>-</sup> ligands thermally exchanged, 1mM **1a** and **2a** were incubated with 500 mM imidazole in buffer (50 mM NaCl, 5 mM Tris pH 7.0) at 37 °C for 16 hours prior to ESI-MS and HPLC analysis.

#### 5. DNA Gel Electrophoresis

Cisplatin, transplatin, **1a**, **1b**, **2a**, and **2b** were serially diluted 1:2 in the presence of 40 μg/mL pUC19 plasmid DNA in 10 mM phosphate buffer, pH 7.4, and incubated

overnight at 37 °C prior to gel electrophoresis. DNA control samples and gel electrophoresis were performed following a previously reported procedure.<sup>1</sup>

## 6. Cell Cytotoxicity

Cytotoxicity of cisplatin, transplatin, **1a**, **1b**, **2a**, and **2b** were determined in HL-60 (human promyelocytic leukemia) and A549 (human lung carcinoma) cell lines. The cell lines were maintained in IMDM media (HL-60) or DMEM media (A549) supplemented with 10% fetal bovine serum (FBS) and 50 U/mL penicillin/streptomycin at 37 °C with 5% CO<sub>2</sub>. For cytotoxicity assays, the cells were plated in Opti-MEM supplemented with 1% FBS and 50 U/mL penicillin/streptomycin at 30,000 cells per well (Costar 96 well flat bottom clear tissue culture treated plates). Each compound was dosed from 0 to 100 μM and incubated for 72 hours. The concentration of DMSO was less than 1% in all cell studies, and no impact is seen on cell viability or behavior at this concentration. Following incubation 73 μM Resazurin was added to each well. The resulting fluorescence was measured and the data was fit to the sigmoidal dose response equation using Prism Software.

## 7. Cellular Uptake

Cellular uptake of **1a** and **2a** were determined in HL-60 cells using graphite furnace atomic absorption spectrometry. The cells were plated in 2 mL of Opti-MEM supplemented with 1% FBS and 50 U/mL penicillin/streptomycin at a density of 1 x 10<sup>6</sup> cells/mL. Compounds **1a** and **2a** were dosed in triplicate at 20 μM and incubated for 12 hours at 37 °C with 5% CO<sub>2</sub>. Following incubation, trypan blue was used to count the number of living and dead cells. The 2 mL cell culture was centrifuged at 1200 rpm for 5 min and 10 μL of the supernatant was transferred to a new microcentrifuge tube. The cell pellet was washed with 1 mL 1X PBS, centrifuged at 1200 rpm for 5 min, decanted, and repeated two times.

The washed cell pellet was resuspended in 480 μL autoclaved MilliQ water and transferred to a 1.5 mL screw cap cryotube, where 120 μL concentrated HNO<sub>3</sub> was added. Simultaneously, 5 μL of the supernatant was transferred to a 1.5 mL screw cap cryotube, where 120 μL concentrated HNO<sub>3</sub> was added. All cryotubes were heated at 110 °C for 3 hours. Upon cooling, samples were analyzed using graphite furnace atomic absorption spectrometry and cellular uptake was determined.

## 8. Additional Tables and Figures

**Table S1.** Conditions for thermal exchange kinetics.

Condition
water
1X phosphate buffer saline (PBS)
Opti-MEM with 1% FBS
50 mM NaCl, 5 mM Tris, pH 7.0

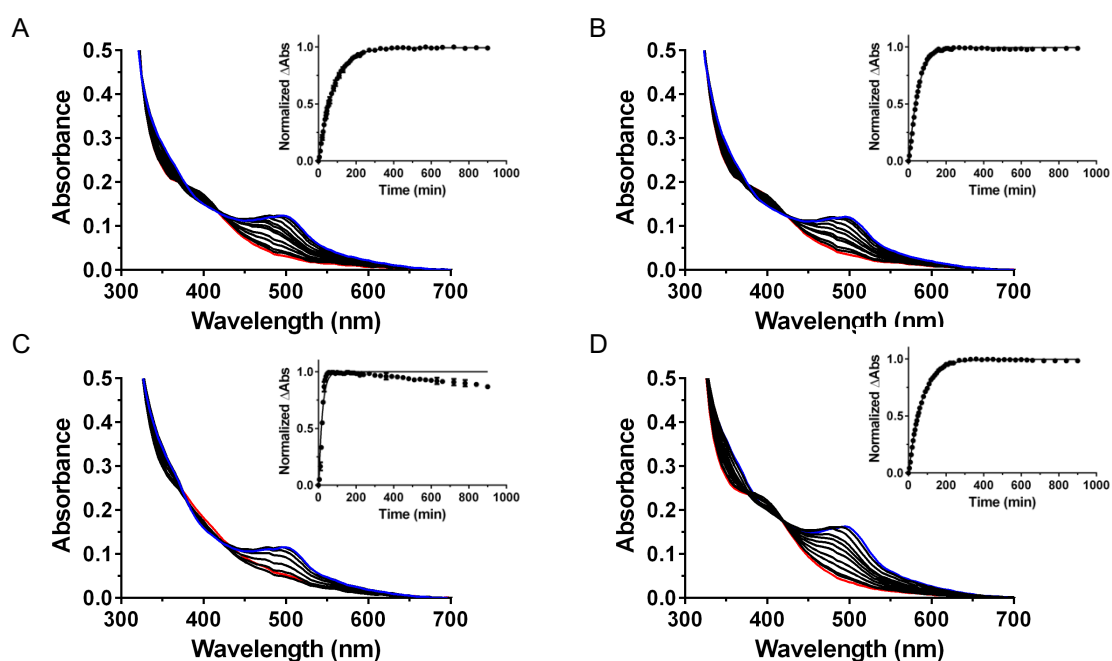


**Figure S1.** Thermal exchange of **1a** (40 μM) followed by UV/Vis absorption spectroscopy in different aqueous solutions. (A) water, (B) 1X PBS, (C) Opti-MEM with 1% FBS, and (D) 50 mM NaCl, 5 mM Tris at pH 7.0; the blue line is  $t = 0$  min and the red line is  $t = 15$  hr. Inset shows the change in absorbance as a function of time fit to a one phase decay equation with Prism software.

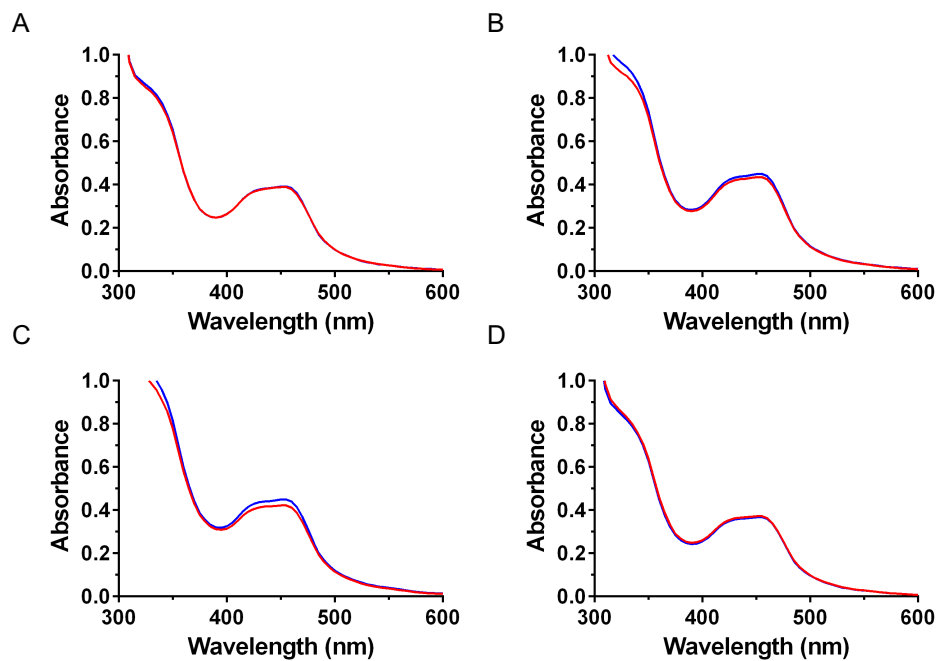


**Figure S2.** Thermal exchange of **1b** (40  $\mu$ M) followed by UV/Vis absorption spectroscopy in different aqueous solutions. (A) water, (B) 1X PBS, (C) Opti-MEM with 1% FBS, and (D) 50 mM NaCl, 5 mM Tris at pH 7.0; the blue line is  $t = 0$  min and the red line is  $t = 15$  hr.

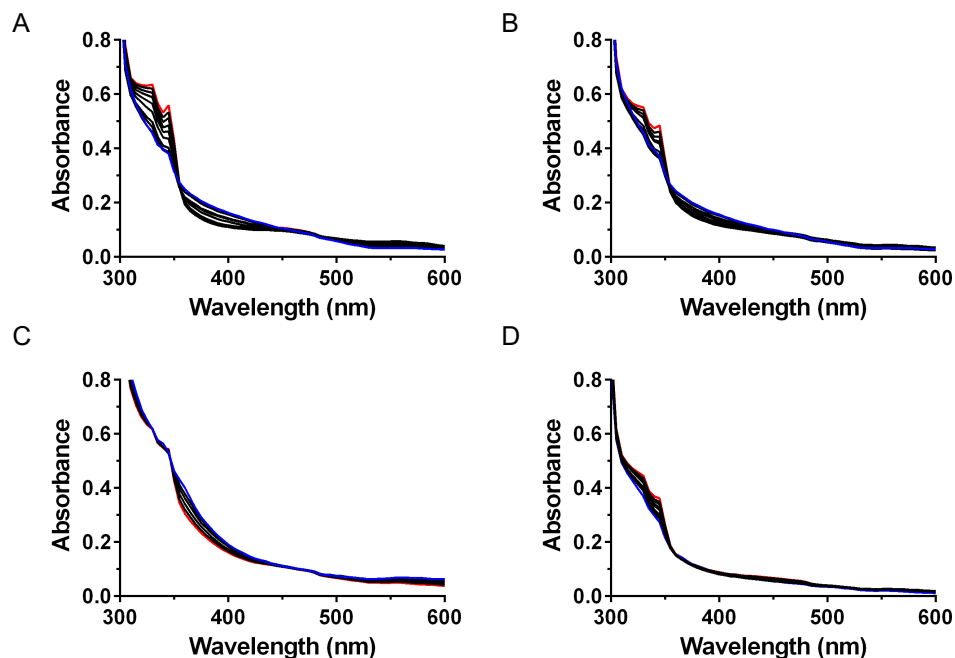


**Figure S3.** Thermal exchange of **2a** (40  $\mu$ M) followed by UV/Vis absorption spectroscopy in different aqueous solutions. (A) water, (B) 1X PBS, (C) Opti-MEM with 1% FBS, and (D) 50 mM NaCl, 5 mM Tris at pH 7.0; the blue line is  $t = 0$  min and the red line is  $t = 15$  hr.

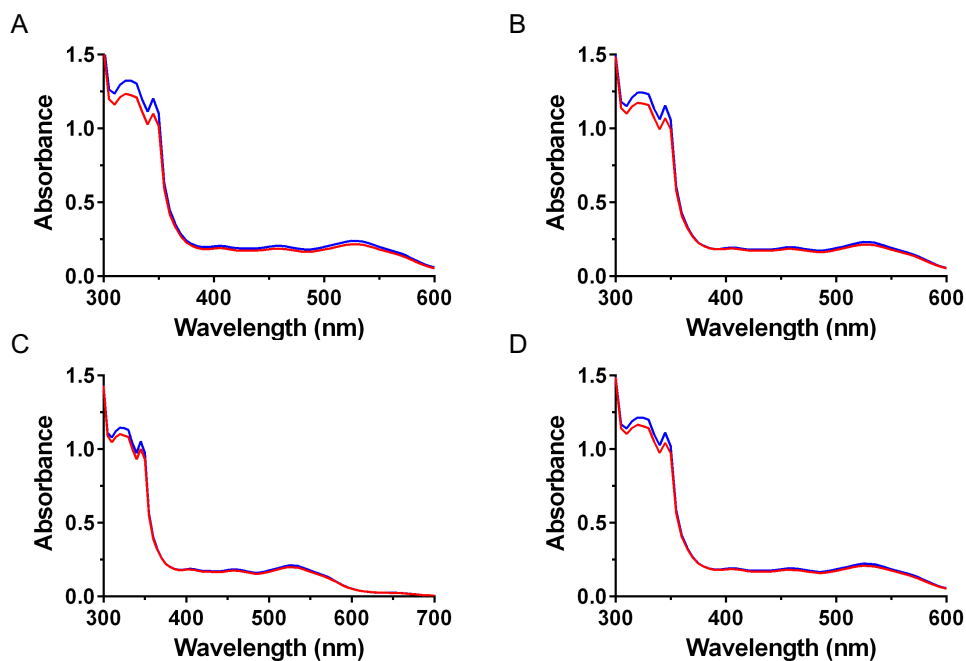


**Figure S4.** Thermal exchange of **2b** (40  $\mu\text{M}$ ) followed by UV/Vis absorption spectroscopy in different aqueous solutions. (A) water, (B) 1X PBS, (C) Opti-MEM with 1% FBS, and (D) 50 mM NaCl, 5 mM Tris at pH 7.0; the blue line is  $t = 0$  min and the red line is  $t = 15$  hr.

**Table S2.** Half-lives of thermal exchange and DNA binding for **1a**.

Condition	$t_{1/2}$ (min)	$\Delta\text{abs @ 500nm}$
water	$53 \pm 3$	$0.085 \pm 0.008$
1X PBS	$33.4 \pm 0.2$	$0.083 \pm 0.005$
Opti-MEM with 1% FBS	$12.8 \pm 0.3$	$0.05 \pm 0.02$
50 mM NaCl, 5 mM Tris, pH 7.0	$48 \pm 1$	$0.13 \pm 0.02$

**Table S3.**  $\Delta\text{abs}$  of thermal exchange and DNA binding for **1b**.

Condition	$\Delta\text{abs @ 450 nm}$
water	$0.0025 \pm 0.0005$
1X PBS	$0.015 \pm 0.001$
Opti-MEM with 1% FBS	$0.021 \pm 0.009$
50 mm NaCl, 5 mm Tris, pH 7.0	$0.013 \pm 0.008$

**Table S4.**  $\Delta_{\text{abs}}$  of thermal exchange and DNA binding for **2a**.

Condition	$\Delta_{\text{abs @ 345 nm}}$
water	$0.19 \pm 0.02$
1X PBS	$0.13 \pm 0.02$
Opti-MEM with 1% FBS	$0.011 \pm 0.003$
50 mM NaCl, 5 mM Tris, pH 7.0	$0.089 \pm 0.005$

**Table S5.**  $\Delta_{\text{abs}}$  of thermal exchange and DNA binding for **2b**.

Condition	$\Delta_{\text{abs @ 325 nm}}$
water	$0.07 \pm 0.03$
1X PBS	$0.06 \pm 0.01$
Opti-MEM with 1% FBS	$0.05 \pm 0.02$
50 mM NaCl, 5 mM Tris, pH 7.0	$0.06 \pm 0.01$

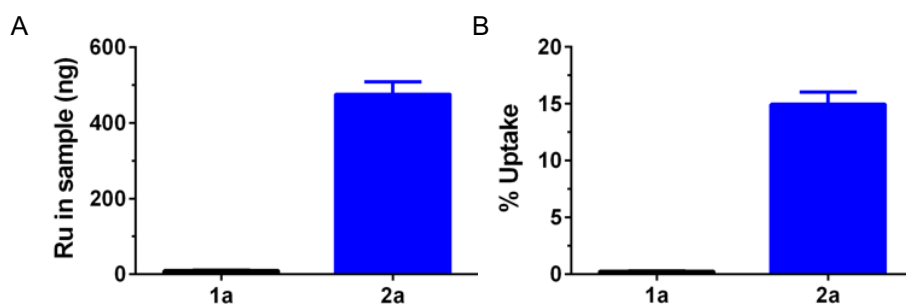


**Figure S5.** Cellular accumulation (A) and % uptake (B) of **1a** (black) and **2a** (blue) in HL-60 cells following a 12 hr incubation as determined by GFAAS.

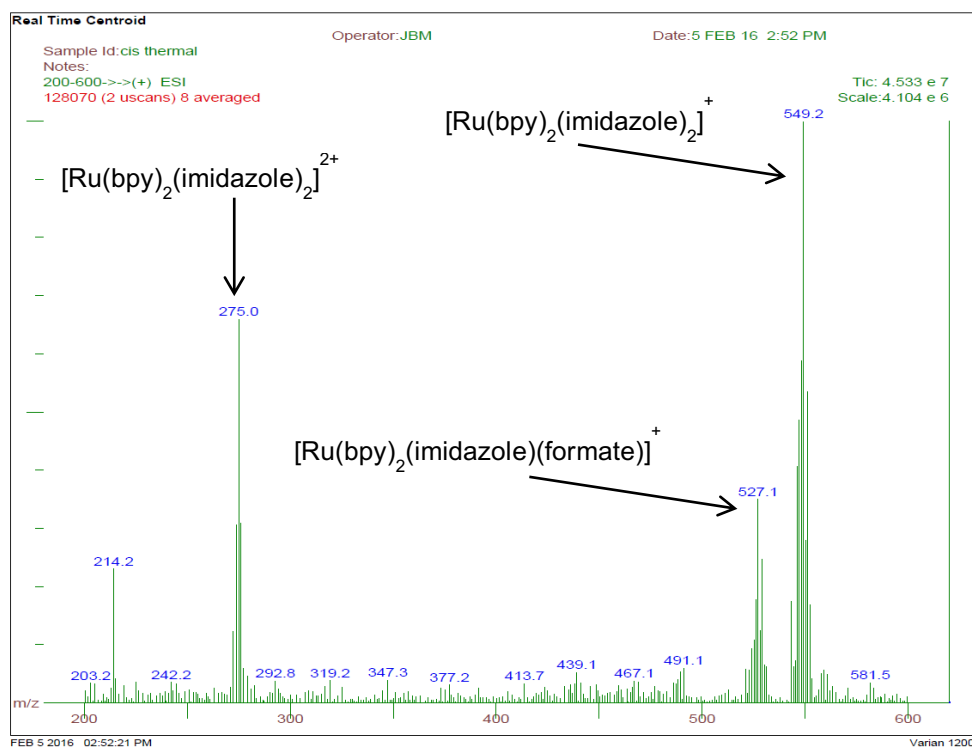


**Figure S6.** ESI-MS for the thermal reaction of **1a** with imidazole. Note: formic acid is used as part of the mobile phase.

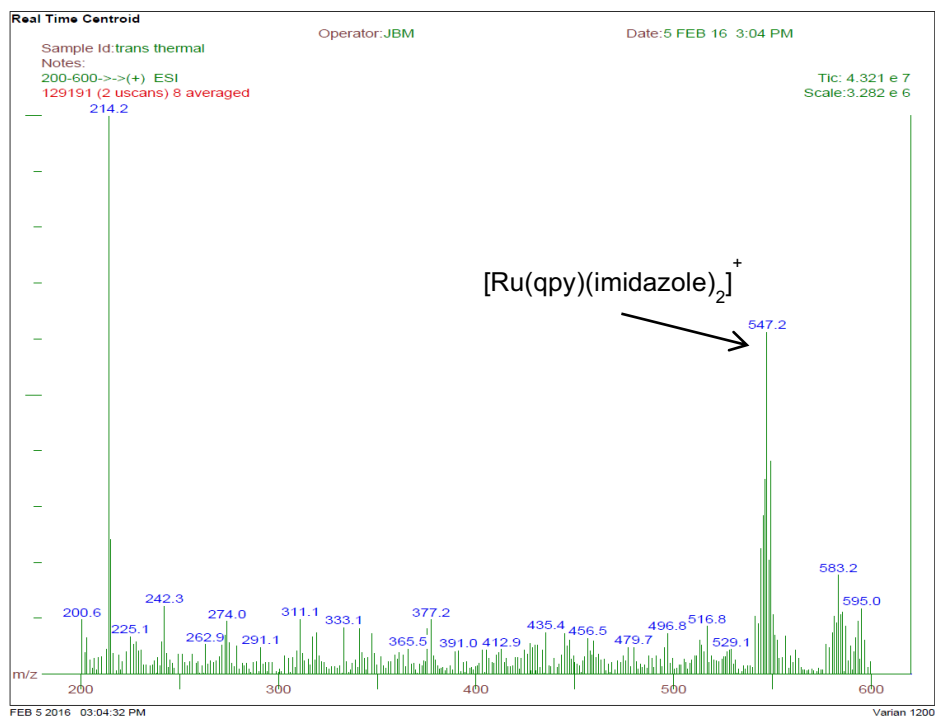


**Figure S7.** ESI-MS for the thermal reaction of **2a** with imidazole. Note: formic acid is used as part of the mobile phase.

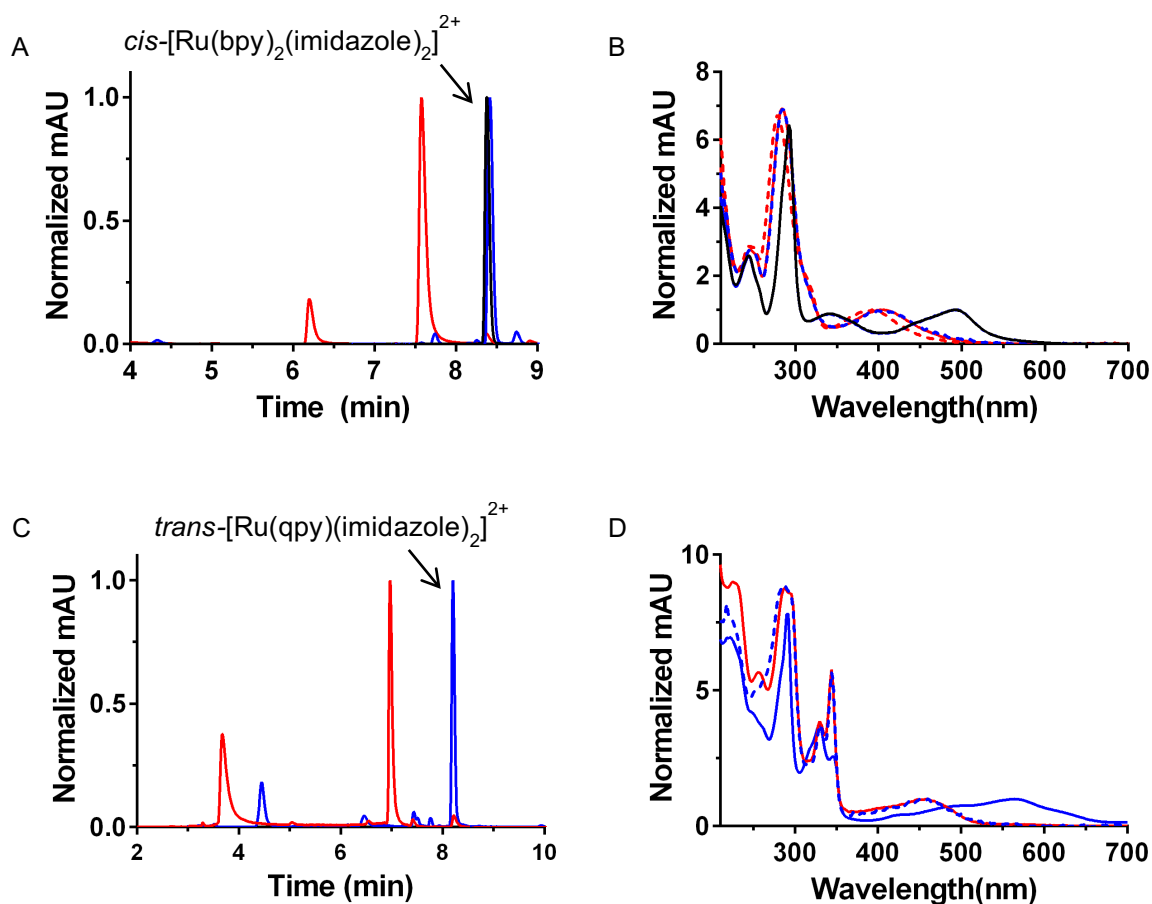


**Figure S8.** HPLC analysis for the thermal reaction of **1a** and **2a** with imidazole. (A) HPLC traces for  $cis\text{-[Ru(bpy)}_2\text{(imidazole)}_2\text{]}^{2+}$  (black), the thermal reaction of **1a** with imidazole (blue), and the thermal reaction of **1a** in buffer only (red). (B) UV/Vis profiles of the peak at 8.4 min for  $cis\text{-[Ru(bpy)}_2\text{(imidazole)}_2\text{]}^{2+}$  (black), the peaks for the thermal reaction of **1a** with imidazole at 8.4 min (blue solid; overlays with the black line, indicate the major product of the thermal reaction of **1a** with imidazole resulted in the formation of  $cis\text{-[Ru(bpy)}_2\text{(imidazole)}_2\text{]}^{2+}$ ). UV/Vis profiles of the peak at 8.8 min (blue dashed), and the peaks for the thermal reaction of **1a** in buffer only at 7.7 min (red solid, overlaying with the blue dashed, indicating the minor product formed in the thermal reaction of **1a** with imidazole is identical to the major product formed in buffer only) and 6.3 min (red dashed, a minor product). (C) HPLC traces for the thermal reaction of **2a** with imidazole (blue) and the thermal reaction of **2a** in buffer only (red). (D) UV/Vis profiles of the peaks for the thermal reaction of **2a** with imidazole at 8.2 min (blue solid), and 4.3 min (blue dashed) and the peak for the thermal reaction of **2a** in buffer only at 7 min (red, overlays with the blue dashed line indicating the minor product formed in the thermal reaction of **2a** with imidazole is identical to the major product formed in buffer only).

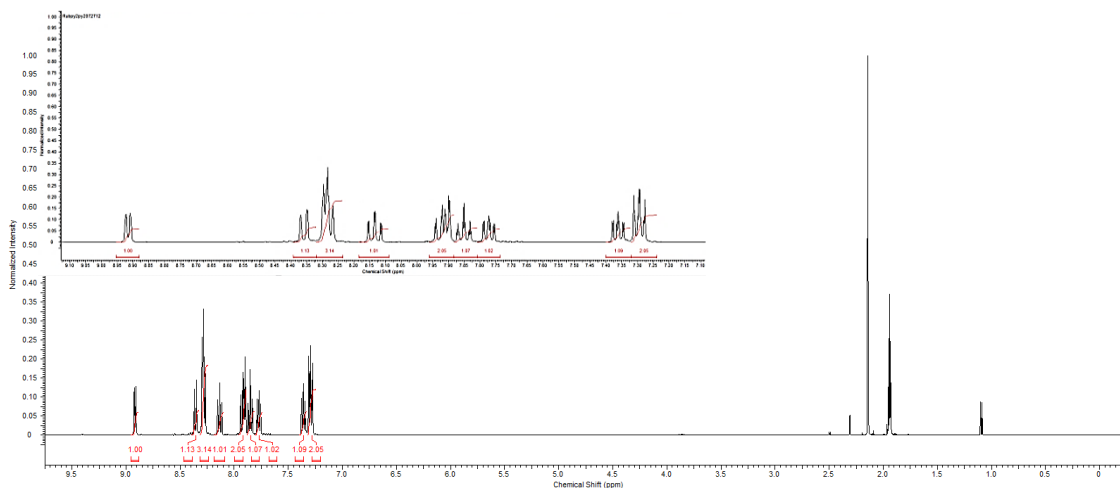


**Figure S9.**  $^1\text{H-NMR}$  in  $\text{CD}_3\text{CN}$  for **1b**

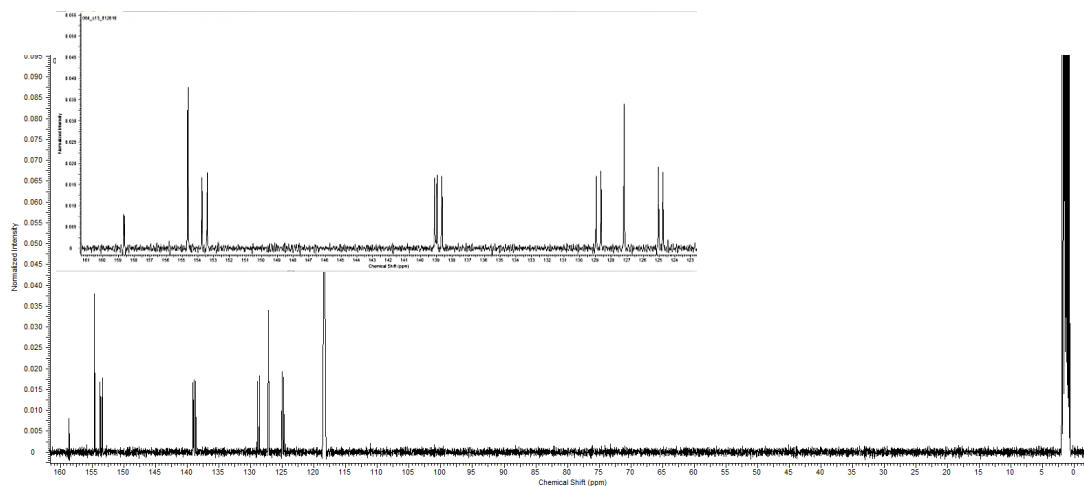


**Figure S10.**  $^{13}\text{C-NMR}$  in  $\text{CD}_3\text{CN}$  for **1b**.

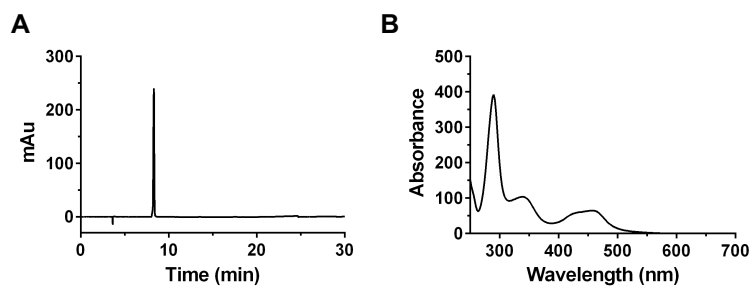


**Figure S11.** HPLC purity (A) and UV/Vis (B) for **1b**

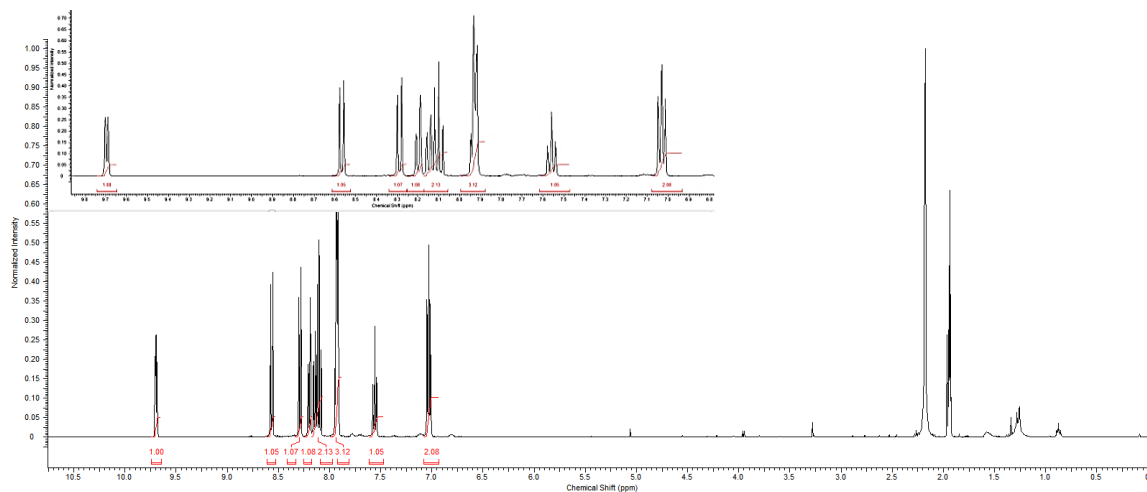


**Figure S12.**  $^1\text{H-NMR}$  in  $\text{CD}_3\text{CN}$  for **2b**.

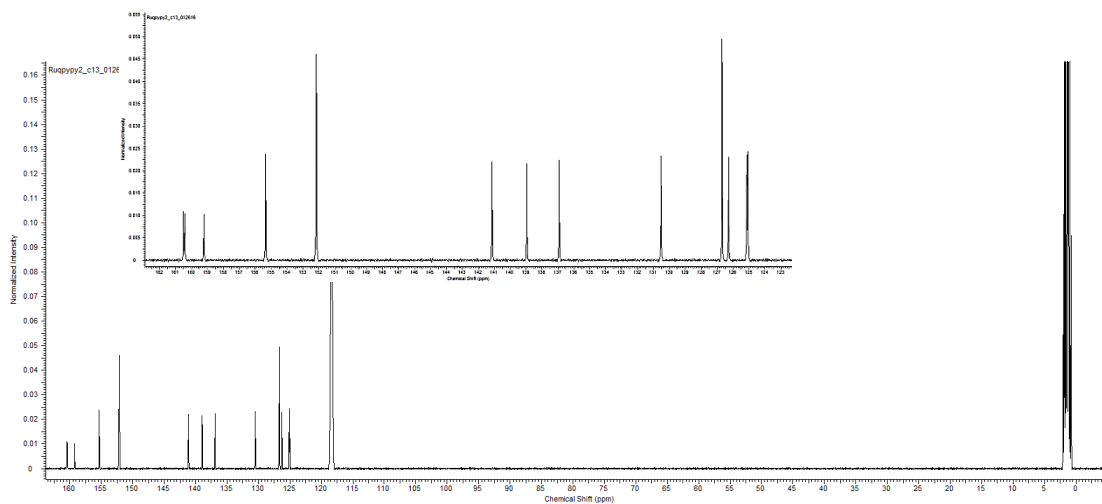


**Figure S13.**  $^{13}\text{C-NMR}$  in  $\text{CD}_3\text{CN}$  for **2b**.

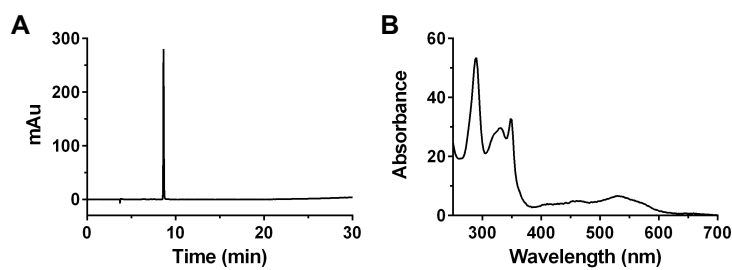


**Figure S14.** HPLC purity (A) and UV/Vis (B) for **2b**.

## 9. References

1. E. Wachter, B. S. Howerton, E. C. Hall, S. Parkin and E. C. Glazer, *Chem. Commun.*, 2014, **50**, 311-313.
2. Y. Liu, S. -M. Ng, S. -M. Yiu, W. W. Lam, X. -G. Wei, K. -C. Lau and T. -C. Lau, *Angew. Chem. Int. Ed. Engl.*, 2014, **53**, 14468-14471.